

Variation of the earth tide –seismicity compliance parameter p the last 17 years for the area of Italy

Arabelos D.N.⁽¹⁾, Contadakis, M.E.⁽¹⁾, Vergos, G.⁽¹⁾, Spatalas, S.⁽¹⁾, Scordilis, E.⁽²⁾

⁽¹⁾ Department of Geodesy and Surveying, University of Thessaloniki, Greece

⁽²⁾ Department of Geophysics, Aristotle University of Thessaloniki, Greece

Abstract: Based on the results of our investigations, which indicate a tidal triggering effect on earthquakes when the stress in the focal area is near the critical level, we prepare yearly maps of the earth tide-seismicity compliance parameter p , for Italy for the years 2000-2016. It is shown that the earth tide-seismicity p maps points to the broader area of pending strong earthquakes within a year with a confidence level of 100%. Thus we suggest that earth tide-seismicity p maps may be used for earthquake risk mitigation

1.Introduction

Applying the Hi(stogram)Cum(ulation) method, which was introduced by Cadicheanu et al. (2007), we analyze the series of the earthquakes occurred in the last 50 years in seismic active areas of Greece, i.e. the areas (a) of the Mygdonian Basin(Contadakis et al. 2007), (b) of the Ionian Islands (Contadakis et al. 2012) and (c) of the Hellenic Arc (Vergos et al. 2012,2015). The result of the analysis for all the areas indicate that the monthly variation of the frequencies of earthquake occurrence is in accordance with the period of the tidal lunar monthly and semi-monthly (Mm and Mf) variations and the same happens with the corresponding daily variations of the frequencies of earthquake occurrence with the diurnal luni-solar (K1) and semidiurnal lunar (M2) tidal variations. In addition the confidence level for the identification of such period accordance between earthquakes occurrence and tidal periods varies with seismic activity, i.e. the higher confidence level corresponds to periods with stronger seismic activity. These results are in favor of a tidal triggering process on earthquakes when the stress in the focal area is near the critical level. Based on these results, we consider the confidence level of earthquake occurrence - tidal period accordance, p , as an index of tectonic stress criticality for earthquake occurrence. Then we construct maps of p 's by analyzing the series of the earthquakes with magnitude $M > 3.0$, which occurred in the last 16 years in Italy ($36^\circ \leq \varphi \leq 48^\circ$, $6^\circ \leq \lambda \leq 19^\circ$) and we check on posterior if the variation of the confidence level index, p , indicate the fault maturity for earthquake occurrence in the case of the recent seismic activity at Central Italy. The result of this test is positive encouraging the inclusion of the following up of the compliance index p in earthquake risk assessment procedure.

2. Seismotectonic features of the Italian Peninsula

Italy is located in one of the most seismically active regions of Europe. Consequently, many strong earthquakes with magnitudes exceeding $M=6.0$ have been occurred in this region with significant consequences. In the map of figure (1) are presented the

epicenters of all known strong ($M \geq 6.0$) earthquakes, which occurred between 1900 and October 2016 in Italy and surroundings.

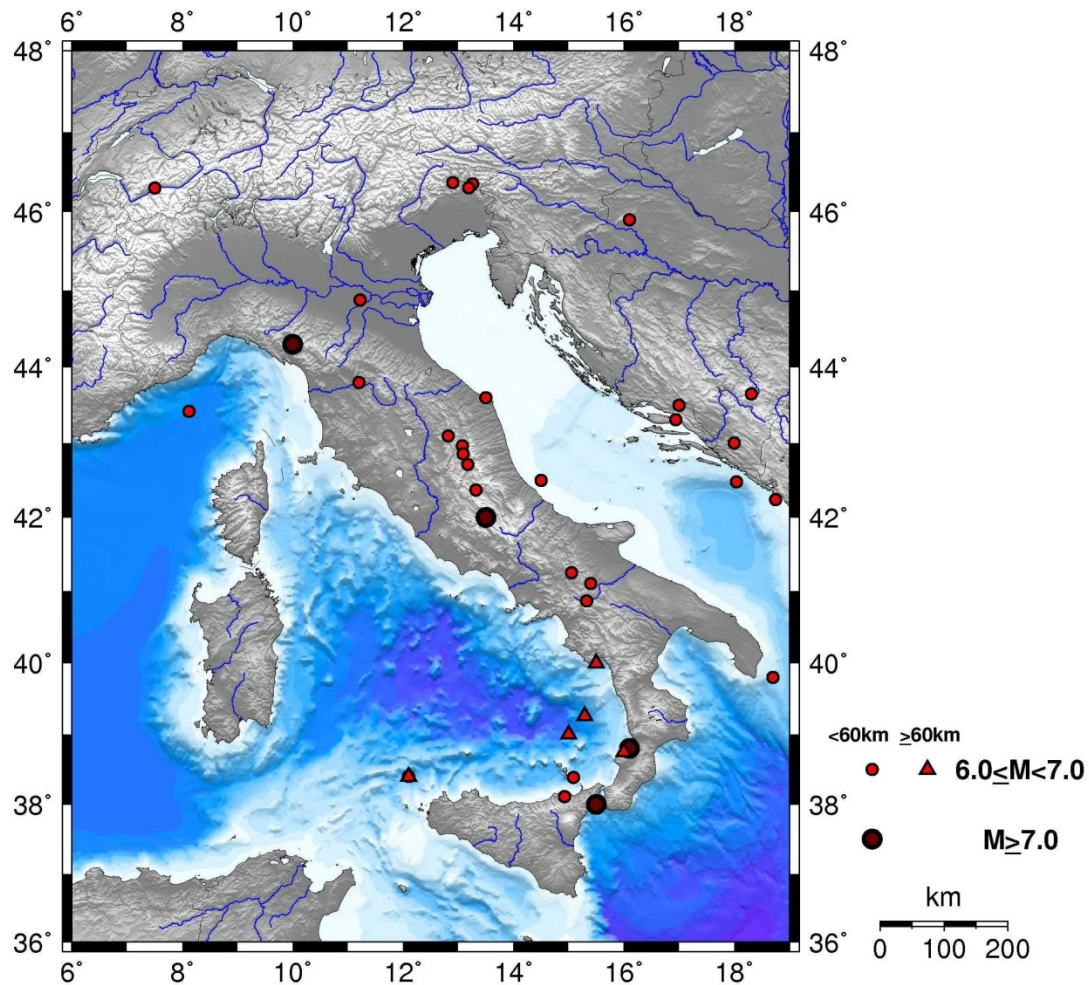


Figure 1. Epicenters of the strongest ($M \geq 6.0$) earthquakes of the Italian peninsula and its surroundings, which occurred during the period 1900-2016(October).

The seismicity in this region is mainly connected with:

- 1) The convergence between African and Eurasian plates, resulting in subduction of Mediterranean under Eurasia. Consequently, a collision takes place between Ionian (front of the Mediterranean plate) and Calabria-Sicily and subduction of the former beneath the latter along the Calabrian arc (e.g. Caputo et al., 1970, 1973; Gasparini et al., 1985; Anderson and Jackson, 1987; Sparkman et al., 1993; Selvaggi and Chiarabba, 1995; Frepoli et al., 1996).
- 2) The continental collision of Adriatic continental lithosphere (micro plate) and Eurasian and its sinking beneath northern Apennines (e.g. Selvaggi and Amato, 1992; Amato et al., 1993; Sparkman et al., 1993).

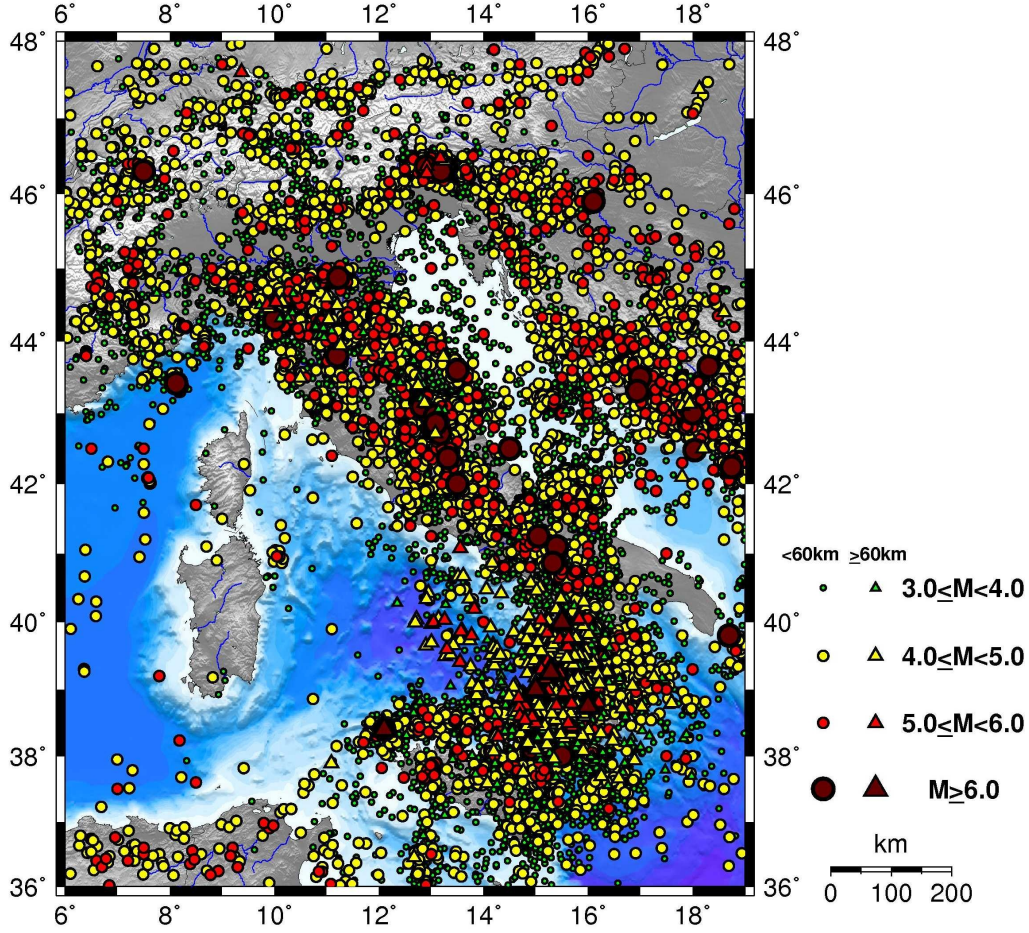


Figure 2. Epicenters of all known earthquakes with $M \geq 3.0$ which occurred in the Italian peninsula and its surroundings, during the period 1900-2016 (October).

As a result, shallow, intermediate depth and deep focus seismicity is observed in the Italian peninsula. A representative picture of the seismicity of the broader area of the Italian peninsula is given in figure (2) that demonstrates the epicenters of all known regional earthquakes with $M \geq 3.0$ which occurred during the period 1900-2016 (October). Most of the epicenters are observed along Apennines and in the region of Calabria-Sicily and correspond to shallow earthquakes, with focal depths within the first 30km. However, intermediate and deep-focus earthquakes are also observed but they are rather sparse and are located beneath northern Apennines and beneath the Calabrian arc (the back-arc regions of the aforementioned plate margins).

In the present study are used the focal parameters of the earthquakes that cover the period 2000-October 2016. Their focal parameters were taken, mainly, from the on-line catalog of the International Seismological Centre (ISC, <http://www.isc.ac.uk>). The area covered is bounded by the coordinates $36^\circ \leq \varphi \leq 48^\circ$, $6^\circ \leq \lambda \leq 19^\circ$ and the minimum magnitude is set to $M=3.0$. To assure homogenization of the catalogue, all magnitudes are expressed in the moment magnitude scale, M_w , and are either adopted (when original estimations were available) or estimated by applying proper relations converting other magnitude scales to M_w (Scordilis 2006; Tsampas, 2006; Duni et al., 2010).

3. Method of Analysis

As we have done in similar studies (Contadakis et al. 2007, Contadakis et al. 2012, Vergos et al. 2012), in order to check the possible correlation between Earth tides and earthquake occurrence we check the time of occurrence of each earthquake in relation to the sinusoidal variation of Earth tides and investigate the possible correlation of the time distribution of the earthquake events with Earth tides variation. Since the periods of the Earth tides component are very well known and quite accurately predictable in the local coordination system we assign a unique phase angle within the period of variation of a particular tidal component, for which the effect of earthquake triggering is under investigation, with the simple relation:

$$\phi_i = \left\{ \left[(t_i - t_0) / T_d \right] \right\} - \text{int} \left\{ \left[(t_i - t_0) / T_d \right] \right\} \times 360 \quad (1)$$

where ϕ_i = the phase angle of the time occurrence of the i earthquake in degrees,

t_i = the time of occurrence of the i earthquake in Modified Julian Days (MJD),

t_0 = the epoch we have chosen in MJD,

T_d = the period of the particular tidal component in Julian Days.

We choose as epoch t_0 , i.e. as reference date, the time of the upper culmination in Thessaloniki of the new moon of January 7, 1989 which has MJD = 47533.8947453704. Thus the calculated phase angle for all the periods under study has 0 phase angle at the maximum of the corresponding tidal component (of course M2 and S2 has an upper culmination maximum every two cycles). As far as the monthly anomalistic moon concern the corresponding epoch t_0 is January 14, 1989 which has MJD = 47541.28492.

We separate the whole period in 12 bins of 30° and stack every event according to its phase angle in the proper bin. Thus we construct a Cumulative Histogram of earthquake events for the tidal period under study.

In order to check the compliance of the earthquake frequency distribution periods with the tidal periods we use the well known Shuster's test (Shuster 1897, see also Tanaka et al. 2002; 2006 and Cadicheanu et al. 2007). In Shuster's test, each earthquake is represented by a unit length vector in the direction of the assigned phase angle \tilde{a}_i . The vectorial sum D is defined as:

$$D^2 = \left(\sum_{i=1}^N \cos a_i \right)^2 + \left(\sum_{i=1}^N \sin a_i \right)^2, \quad (2)$$

where N is the number of earthquakes. When a_i is distributed randomly, the probability to be the length of a vectorial sum equal or larger than D is given by the equation:

$$p = \exp \left(-\frac{D^2}{N} \right) \quad (3)$$

Thus, $p < 5\%$ represents the significance level at which the null hypothesis that the earthquakes occurred randomly with respect to the tidal phase is rejected. This means

that the smaller the p is the greater the confidence level of the results of the Cumulative Histograms is. Finally it should be noted that the total number of the shocks for each year is greater than 30 for all the years. This means that the normal distribution approach on which Shuster test is based is valid for all the years.

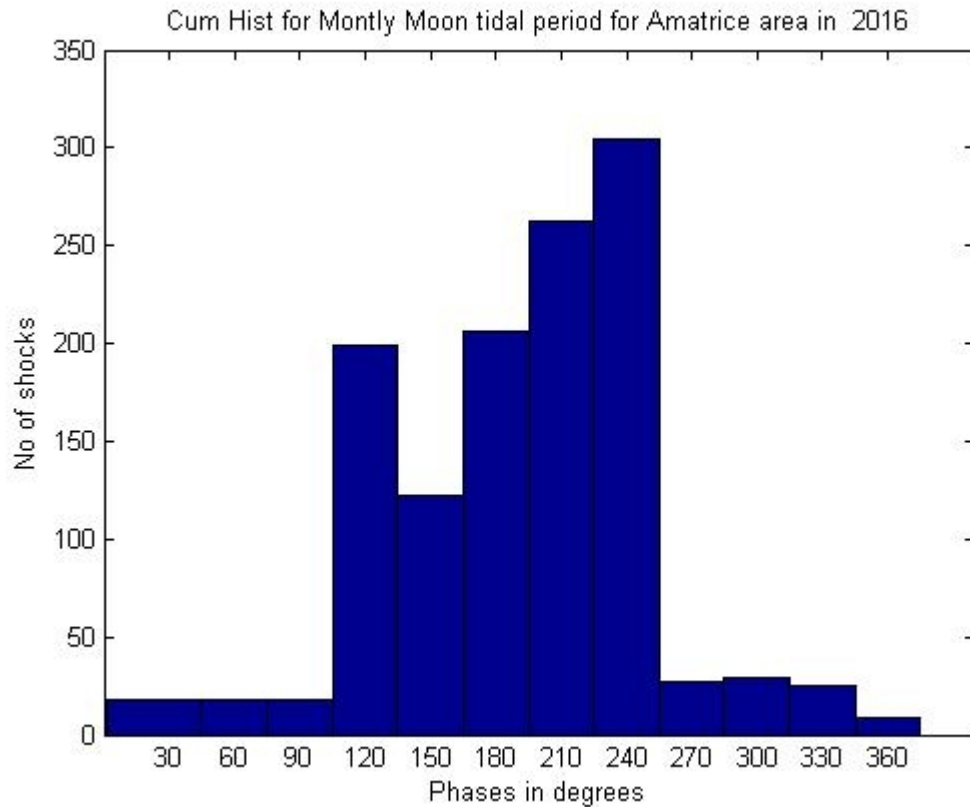


Figure 3. Cumulation Histogram for the Synodic Monthly period for 2016, for the Amatrice Area

As an example Figure 3 display the Cumulation Histogram for the Synodic Monthly period for the earthquakes of the Amatrice area in the year 2016. The earth tide-seismicity compliance parameter p for this tidal period is 0.0, i.e. there is perfect compliance.

4. The compliance parameter p maps

Figures 4 to 20 display the earth tide-seismicity compliance parameter p maps for the years 2000-2016 for the area of Italy. The compliance parameter p was deduced from the Compliance parameter p of the Lunar Monthly Synodic tidal period because it has been found in our studies that this index is more sensitive to the seismicity (Contadakis et al. 2007, Contadakis et al. 2012 Vergos et al. 2012).

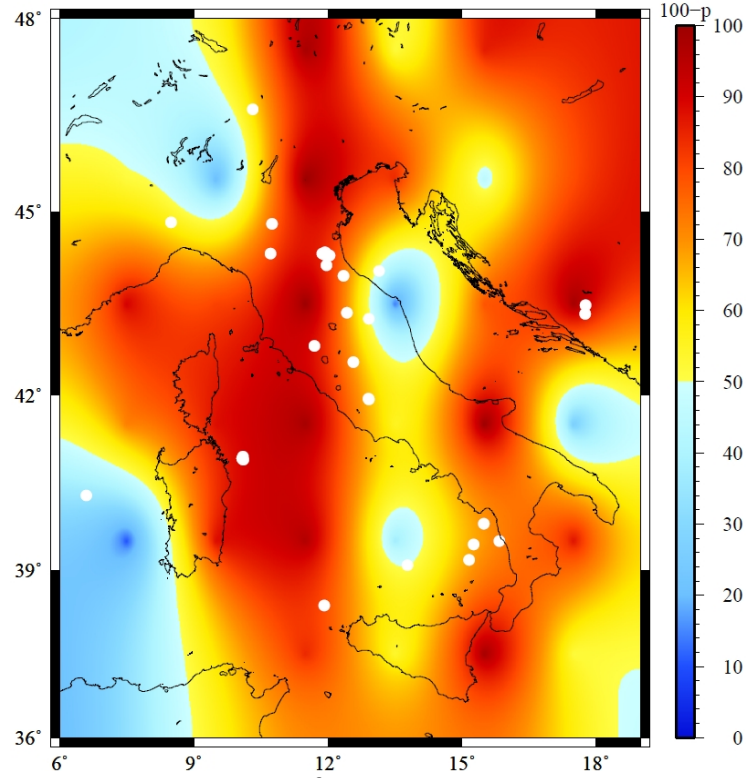


Figure 4. Compliance parameter p of the Lunar Monthly Synodic tidal period for the year 2000. White marks indicate Earthquake epicenters: circles $4.5 < M < 5.5$, stars $M \geq 5.5$.

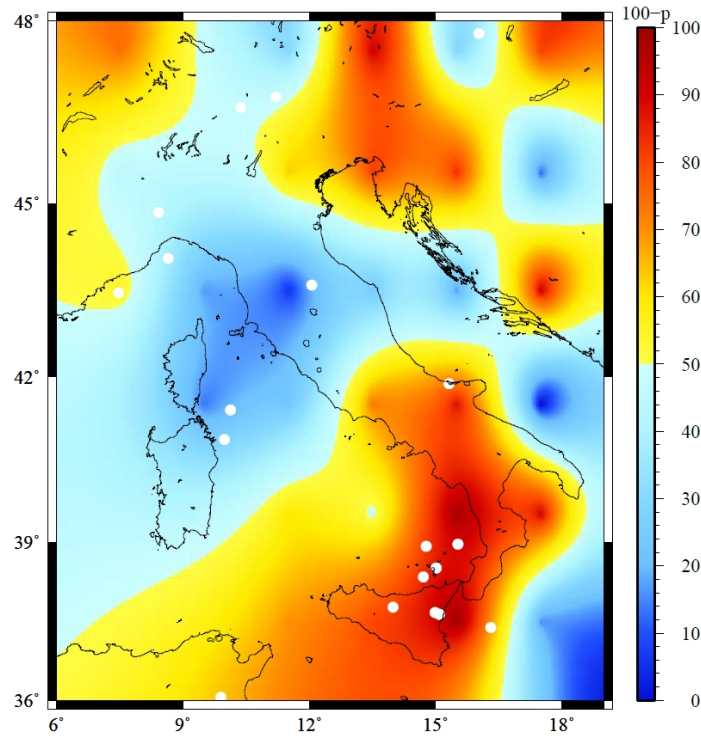


Figure 5. Compliance parameter p of the Lunar Monthly Synodic tidal period for the year 2001. White marks indicate Earthquake epicenters: circles $4.5 < M < 5.5$, stars $M \geq 5.5$.

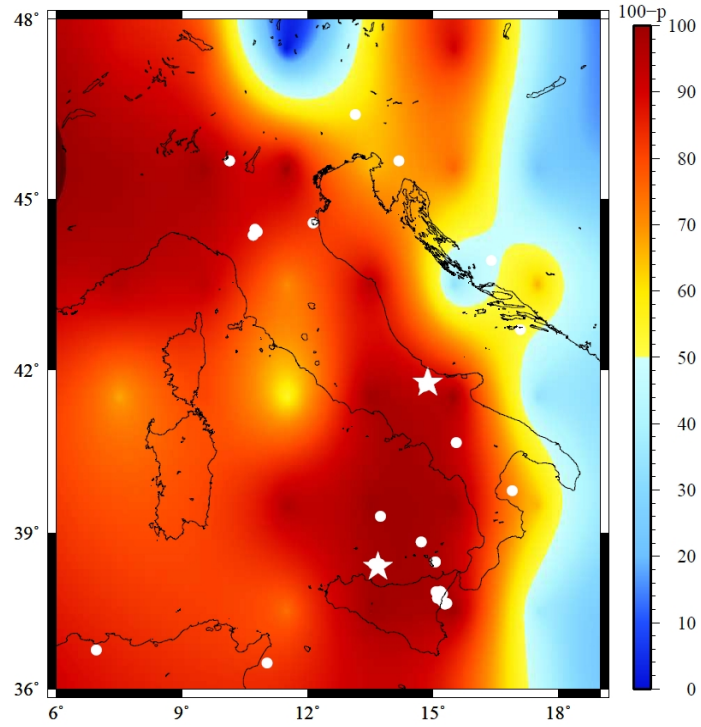


Figure 6. Compliance parameter p of the Lunar Monthly Synodic tidal period for the year 2002. White marks indicate Earthquake epicenters: circles $4.5 < M < 5.5$, stars $M \geq 5.5$.

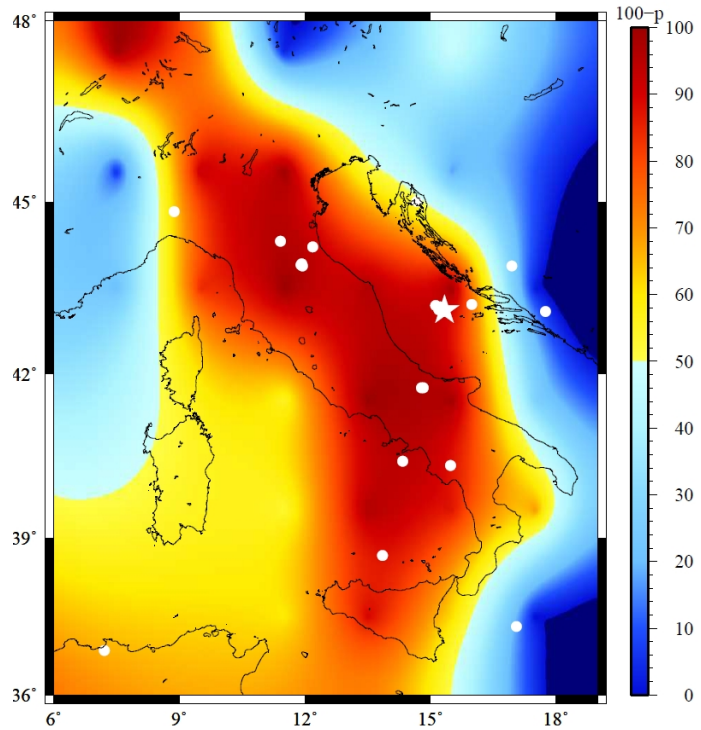


Figure 7. Compliance parameter p of the Lunar Monthly Synodic tidal period for the year 2003. White marks indicate Earthquake epicenters: circles $4.5 < M < 5.5$, stars $M \geq 5.5$.

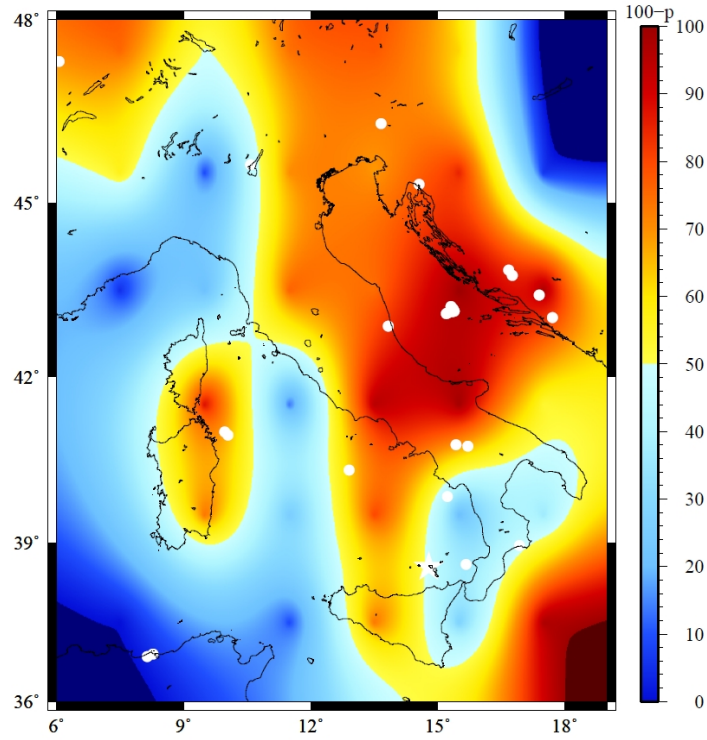


Figure 8. Compliance parameter p of the Lunar Monthly Synodic tidal period for the year 2004. White marks indicate Earthquake epicenters: circles $4.5 < M < 5.5$, stars $M \geq 5.5$.

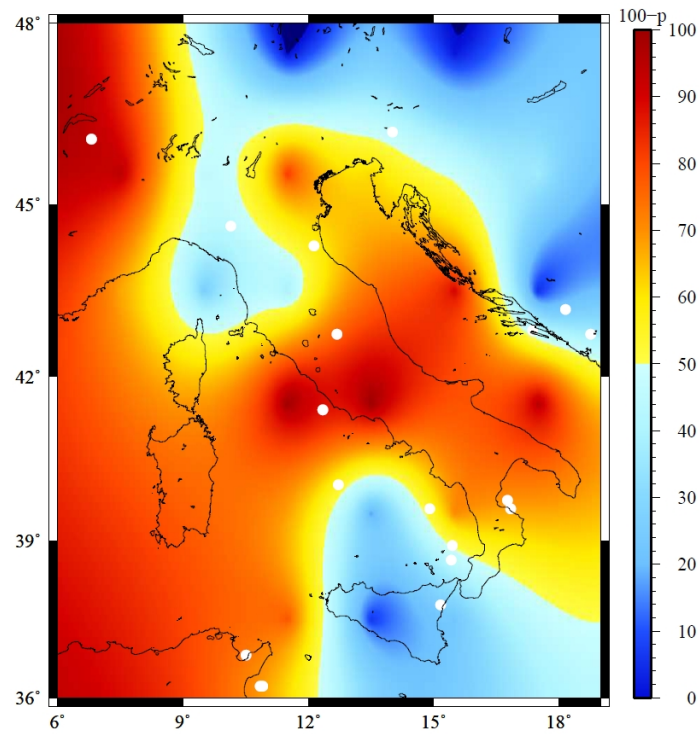


Figure 9. Compliance parameter p of the Lunar Monthly Synodic tidal period for the year 2005. White marks indicate Earthquake epicenters: circles $4.5 < M < 5.5$, stars $M \geq 5.5$.

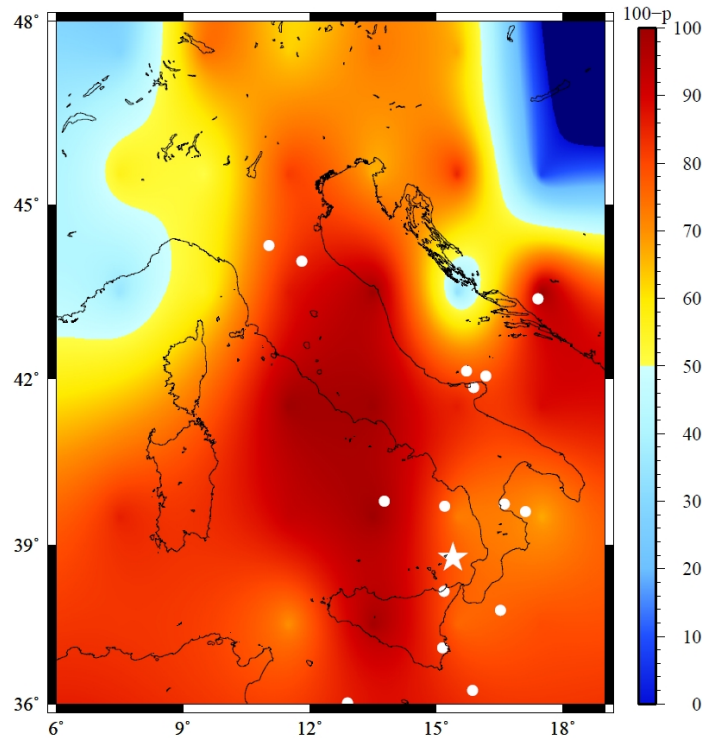


Figure 10. Compliance parameter p of the Lunar Monthly Synodic tidal period for the year 2006. White marks indicate Earthquake epicenters: circles $4.5 < M < 5.5$, stars $M \geq 5.5$.

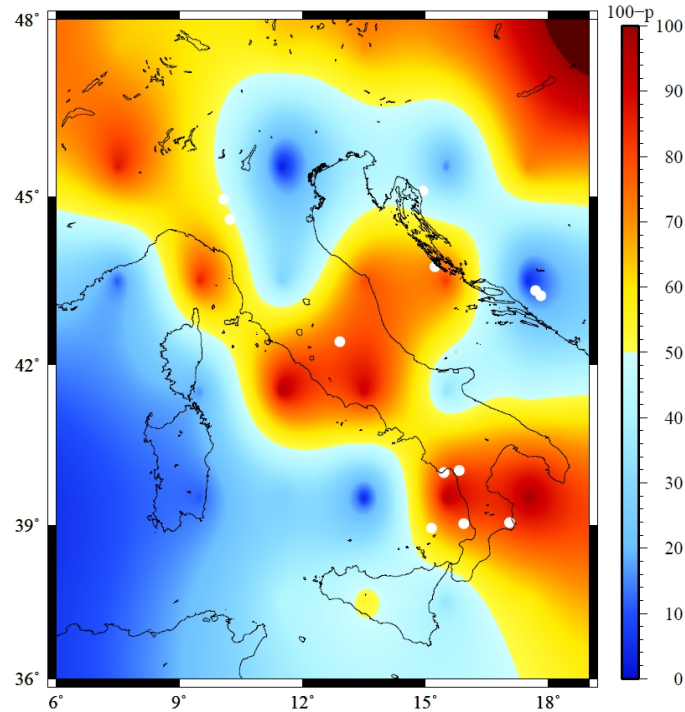


Figure 11. Compliance parameter p of the Lunar Monthly Synodic tidal period for the year 2007. White marks indicate Earthquake epicenters: circles $4.5 < M < 5.5$, stars $M \geq 5.5$.

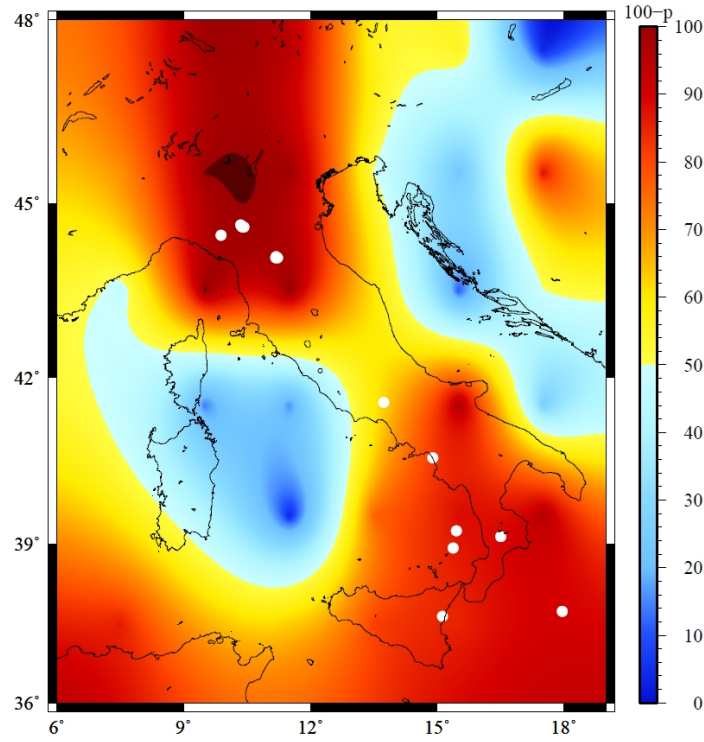


Figure 12. Compliance parameter p of the Lunar Monthly Synodic tidal period for the year 2008. White marks indicate Earthquake epicenters: circles $4.5 < M < 5.5$, stars $M \geq 5.5$.

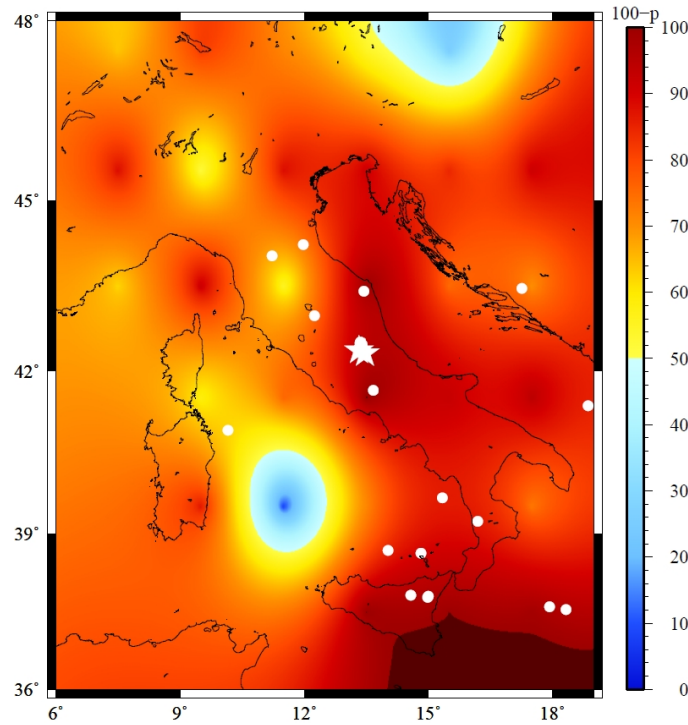


Figure 13. Compliance parameter p of the Lunar Monthly Synodic tidal period for the year 2009. White marks indicate Earthquake epicenters: circles $4.5 < M < 5.5$, stars $M \geq 5.5$.

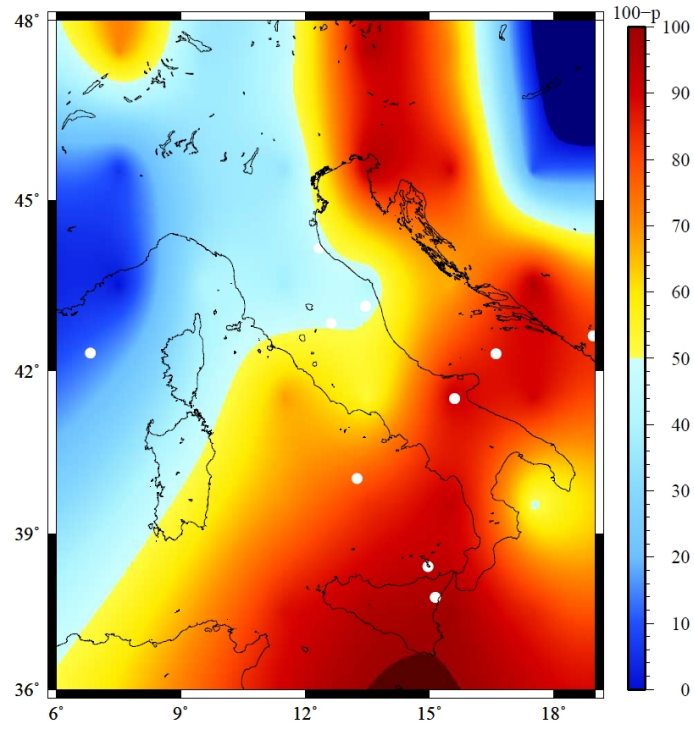


Figure 14. Compliance parameter p of the Lunar Monthly Synodic tidal period for the year 2010. White marks indicate Earthquake epicenters: circles $4.5 < M < 5.5$, stars $M \geq 5.5$.

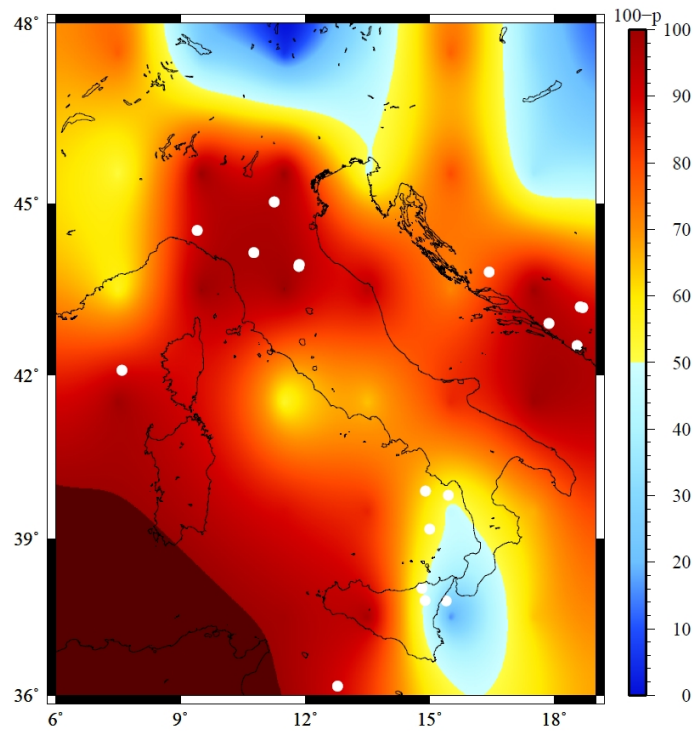


Figure 15. Compliance parameter p of the Lunar Monthly Synodic tidal period for the year 2011. White marks indicate Earthquake epicenters: circles $4.5 < M < 5.5$, stars $M \geq 5.5$.

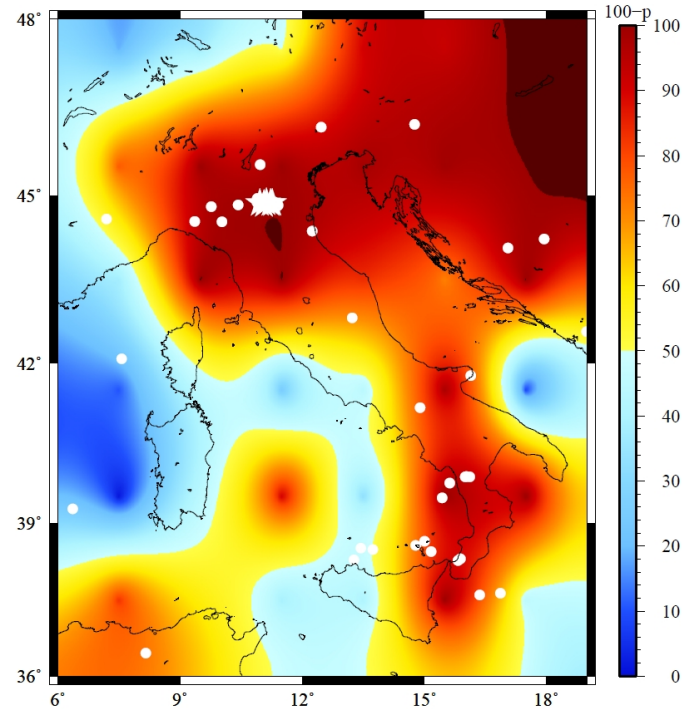


Figure 16. Compliance parameter p of the Lunar Monthly Synodic tidal period for the year 2012. White marks indicate Earthquake epicenters: circles $4.5 < M < 5.5$, stars $M \geq 5.5$.

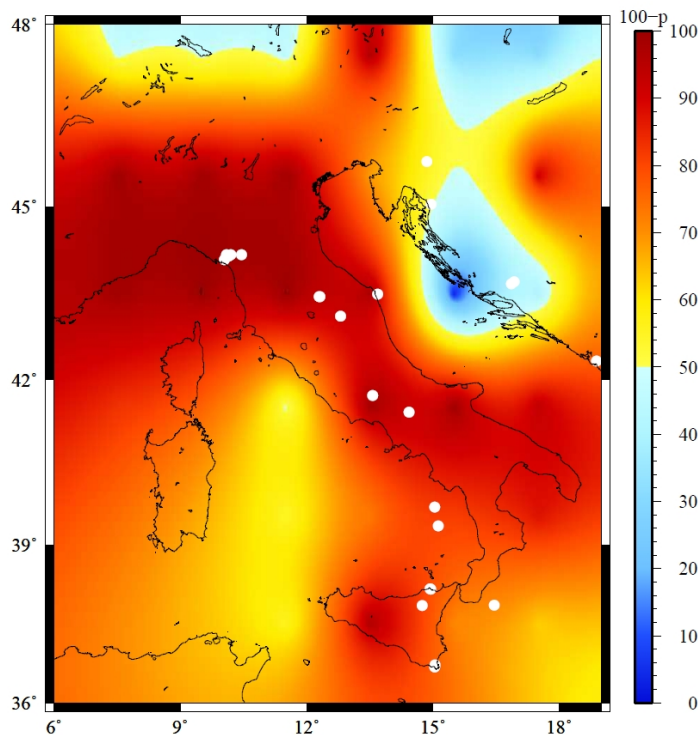


Figure 17. Compliance parameter p of the Lunar Monthly Synodic tidal period for the year 2013. White marks indicate Earthquake epicenters: circles $4.5 < M < 5.5$, stars $M \geq 5.5$.

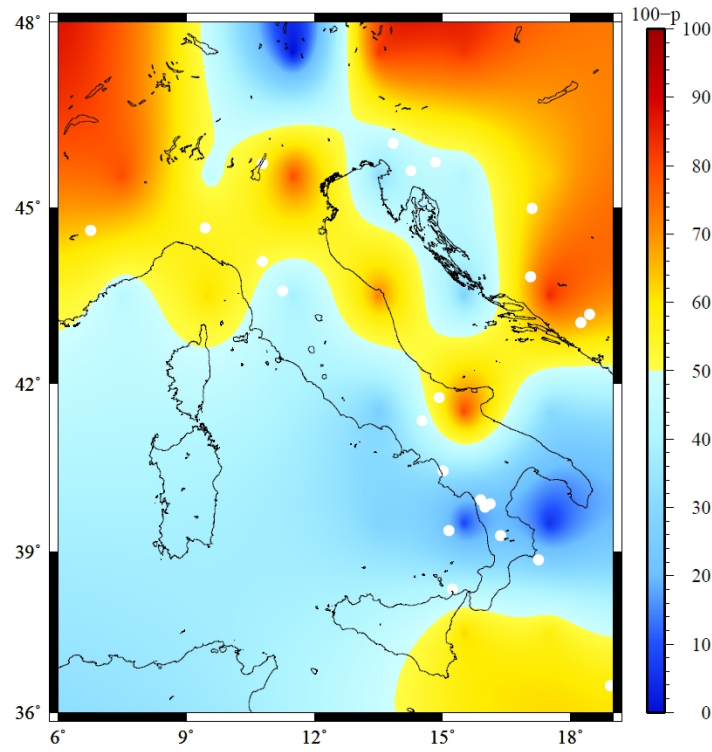


Figure 18. Compliance parameter p of the Lunar Monthly Synodic tidal period for the year 2014. White marks indicate Earthquake epicenters: circles $4.5 < M < 5.5$, stars $M \geq 5.5$.

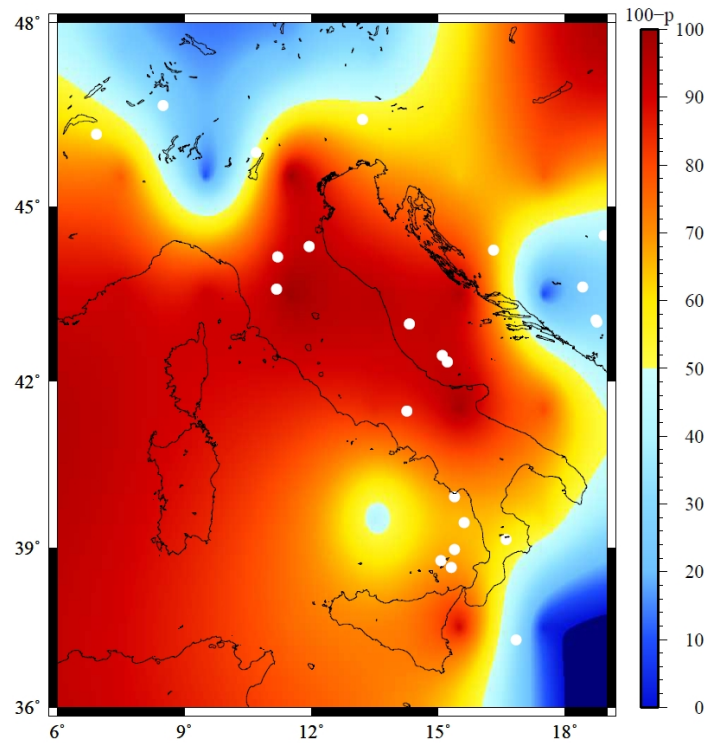


Figure 19. Compliance parameter p of the Lunar Monthly Synodic tidal period for the year 2015. White marks indicate Earthquake epicenters: circles $4.5 < M < 5.5$, stars $M \geq 5.5$.

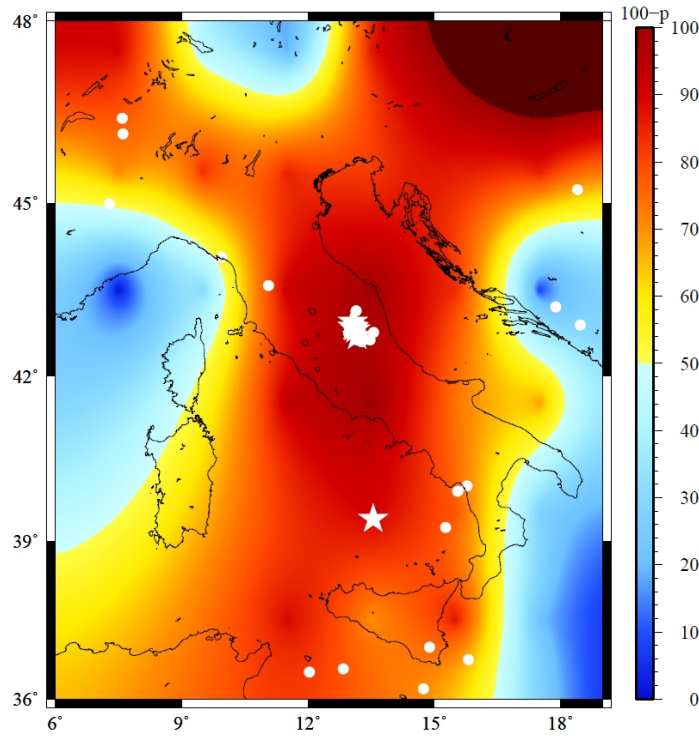


Figure 20. Compliance parameter p of the Lunar Monthly Synodic tidal period for the year 2016. White marks indicate Earthquake epicenters: circles $4.5 < M < 5.5$, stars $M \geq 5.5$.

. From these maps it is realized that the earth tide-seismicity compliance parameter p points to the broader area of significant earthquakes ($M \geq 4.5$) with a very high consistency. More precisely, in these years in the broader area of Aegean occurred 259 significant earthquakes ($M \geq 4.5$) and 13 of them were strong earthquakes ($M \geq 5.5$). The p map failed to point the broader area of 46 epicenter of earthquakes with $4.5 < M < 5.5$. This means that with the help of p maps the broader area of pending strong earthquakes within a year can be determined with a confidence level of 100% and for all the shocks with $M > 4.5$ with a confidence level 82.5%. Thus we suggest that earth tide-seismicity compliance parameter p maps may be used for earthquake risk mitigation.

4. Concluding remarks

In this paper it is shown that the earth tide-seismicity p maps points to the broader area of pending strong earthquakes within a year with a confidence level of 100%. Thus we suggest that earth tide-seismicity p maps may be used for earthquake risk mitigation.

References

Amato, a., B. Alessandrini, G.B. Cimini, A. Frepoli and G. Selvaggi, 1993. Active and remnant subducted slabs beneath Italy: evidence from seismic tomography and seismicity. *Ann. Geofys.*, 36 (2), 201-214.

- Anderson, H.J. and J. Jackson, 1987. The deep seismicity of the Tyrrhenian Sea. *J. R. Astron. Soc.*, 91, 613-637.
- Caputo, M., G.F. Panza and D. Postpischl, 1970. Deep structure of the Mediterranean basin. *J. Geophys. Res.*, 75, 4919-4923.
- Caputo, M., G.F. Panza and D. Postpischl, 1973. New evidences about the deep structure of the Lipari arc. *Tectonophysics*, 15, 219-231.
- Cadicheanu, N., van Ruymbeke, M and Zhu P., 2007: Tidal triggering evidence of intermediate depth earthquakes in Vrancea zone (Romania), *NHESS* 7, 733-740.
- [Contadakis, M. E.](#), [Arabelos, D. N.](#), [Spatalas, S.](#), 2009, Evidence for tidal triggering on the shallow earthquakes of the seismic area of Mygdonia basin, North Greece, in *Terrestrial and Stellar Environment*, eds. D. Arabelos, M.E. Contadakis, C. Kaltsikis, I. Tziavos, Ziti Press Thessaloniki, Greece, pp 223-235
- [Contadakis, M. E.](#), [Arabelos, D. N.](#), [Spatalas, S. D.](#), 2012, Evidence for tidal triggering for the earthquakes of the Ionian geological zone, Greece, *Annals of Geophysics*, Vol. 55, No. 1, p. 73-81
- Duni, L., Sh. Kuka and N. Kuka, 2010. Local relations for converting M_L to M_W in southern-western Balkan region. *Acta Geod. Geoph. Hung.*, 45(3), 317-323.
- Frepoli, A., G. Selvaggi, C. Chiarabba and A. Amato, 1996. State of stress in the southern Tyrrhenian subduction zone from fault-plane solutions. *Geophys. J. Int.*, 125, 879-891.
- Gasparini, C., Iannaccone, G. and Scarpa, R., 1985, Fault-plane solutions and seismicity of the Italian peninsula. *Tectonophysics*, 117, pp. 59-78.
- Scordilis, E.M., 2006. Empirical global relations converting M_s and m_b to moment magnitude. *J. Seismol.*, 10, 225-236.
- Schuster, A., 1897, On lunar and solar periodicities of earthquakes, *Proc. R. Soc. Lond.*, 61, 455-465.
- Selvaggi, G., and Amato, A., 1992, Subcrustal earthquakes in the northern Apennines (Italy): Evidence for a still active subduction? *Geophys. Res. Lett.*, 19, 2127-2130.
- Tanaka, S., Ohtake, M., and Sato, H. 2002, Evidence for tidal triggering of earthquakes as revealed from statistical analysis of global data. *J. Geophys. Res.*, 107(5B10), 2211.
- Tanaka, S., Sato, Matsumura, S., and H., Ohtake, M. , 2006, Tidal triggering of earthquakes in the subducting Philippine Sea plate beneath the locked zone of the plate interface in Tokai region, Japan. *Tectonophysics*, 417, 69-80.
- G. Vergos, D.N. Arabelos, M.E. Contadakis, 2015, Evidence for tidal triggering on the earthquakes of the Hellenic Arc, *Physics and Chemistry of the Earth* 85-86, 210-215
- [Vergos, G.](#), [Arabelos, D. N.](#), [Contadakis, M. E.](#), 2012, Evidence for Tidal triggering on the earthquakes of the Hellenic Arc, Greece., *Geoph. Res. Abs.*, Vol 14, 2325